AD-A130 663 CONVERGENCE OF MODAL SERIES IN A PLATE STRUCK BY A SHOCK WAVE(U) NAVAL RESEARCH LAB WASHINGTON DC R S SCHECHTER ET AL. 21 JUL 83 NRL-MR-5142 1/1

UNCLASSIFIED F/G 13/10 NL

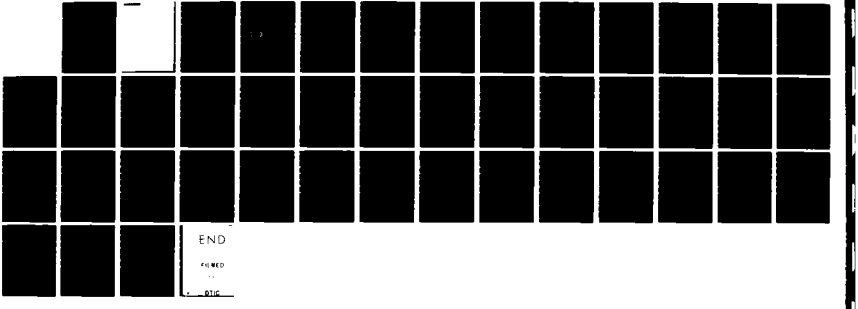

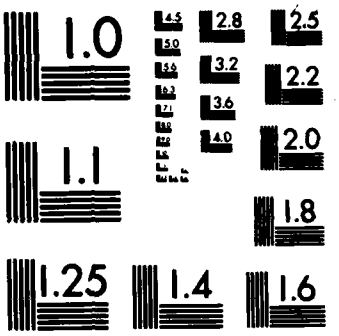

SECURITY CLASSIFICATION OF THIS PAGE (When Data Entered)

REPORT DOCUMENTATION PAGE		READ INSTRUCTIONS BEFORE COMPLETING FORM
1. REPORT NUMBER NRL Memorandum Report 5142	2. GOVT ACCESSION NO. AD-A130663	3. RECIPIENT'S CATALOG NUMBER
4. TITLE (and Subtitle) CONVERGENCE OF MODAL SERIES IN A PLATE STRUCK BY A SHOCK WAVE		5. TYPE OF REPORT & PERIOD COVERED Progress report covering period Nov. 1981 to Apr. 1982. 6. PERFORMING ORG. REPORT NUMBER
7. AUTHOR(s) R. S. Schechter and R. L. Bort		8. CONTRACT OR GRANT NUMBER(s)
9. PERFORMING ORGANIZATION NAME AND ADDRESS Naval Research Laboratory Washington, DC 20375		10. PROGRAM ELEMENT, PROJECT, TASK AREA & WORK UNIT NUMBERS 58-0269-0-0
11. CONTROLLING OFFICE NAME AND ADDRESS David W. Taylor Naval Ship R & D Center Bethesda, Maryland 20084		12. REPORT DATE July 21, 1983 13. NUMBER OF PAGES 42
14. MONITORING AGENCY NAME & ADDRESS(if different from Controlling Office)		15. SECURITY CLASS. (of this report) UNCLASSIFIED 15a. DECLASSIFICATION/DOWNGRADING SCHEDULE

16. DISTRIBUTION STATEMENT (of this Report)

Approved for public release; distribution unlimited.

17. DISTRIBUTION STATEMENT (of the abstract entered in Block 20, if different from Report)

18. SUPPLEMENTARY NOTES

19. KEY WORDS (Continue on reverse side if necessary and identify by block number)

Beam
Plate
Underwater explosion
Submarine appendage

20. ABSTRACT (Continue on reverse side if necessary and identify by block number)

Numerical calculations are shown for a simplified model of a plate subjected to a pressure pulse and a base motion while immersed in an acoustic fluid. Modal series for deflection and velocity converged promptly, but it was found that 20 thin-beam modes were needed to represent time-history bending stresses along the length of a particular steel plate mounted as a cantilever immersed in sea water. A criterion is proposed for

(Continues)

DD FORM 1 JAN 73 1473 EDITION OF 1 NOV 65 IS OBSOLETE
S/N 0102-014-6601

SECURITY CLASSIFICATION OF THIS PAGE (When Data Entered)

20. ABSTRACT (Continued)

calculation of stresses in fluid-structure interactions: the structure must be modeled in enough detail so that individual motions are controlled by stiffness of the structure, with less than 20 percent of critical damping from acoustic radiation.

CONTENTS

CONVERGENCE OF MODAL SERIES IN A PLATE STRUCK BY A SHOCK WAVE

INTRODUCTION

This report continues a sequence of reports on numerical investigations of simple cases in the dynamic responses of structures to transient loadings. The objective of the investigations has been to develop insight into the behavior of structures under dynamic loadings by considering cases which are simple enough to be exhaustively analyzed but which contain the essential features of some complex problem which is of real interest.

The problem of present concern is the effect of underwater-explosion attacks on appendages or external structures of combat submarines. An underwater explosion produces a pulse of pressure which may damage the sail, rudder, diving plane, or other appendage of a submarine directly as it sweeps around it or through it, or which may damage it as a result of shock motions which it produces in the section of the hull to which the appendage is attached. A prediction of the peak stress produced in the structure of an appendage by a given pressure pulse or base motion would seem to be a useful step in assessing the danger that an appendage might be distorted enough to become inoperable, or be blown away entirely, by an underwater-explosion attack. Such stresses can be calculated by modeling the structure as an array of finite elements, applying loads, and calculating responses directly on a high-speed computer.

Minimum essential features of the problem are seen to be a representation of the structure, a representation of the surrounding water as it interacts with the structure, and provisions for loading by means of a pressure pulse or a base motion. The minimum features were incorporated here by considering a thin rectangular plate cantilevered from a moving base and surrounded by an acoustic fluid. The complexity of a usual structural model was simulated by supposing that the plate could respond in multiple modes of plane-strain bending and the effects of the fluid were simulated by simple plane-wave interactions. More-general methods of modeling structures and representing fluid-structure interactions can be considered as elaborations of the simple methods described here.

Results shown here indicate that acoustic damping, as provided by the surrounding fluid, seems to destablilize the calculations by causing stresses and strains to increase with increasing frequency or increasingly-elaborate finite-element representations of the structure. It appears to be necessary to carry the structural representation up to the range of detail where the response is no longer controlled by damping in order to obtain valid estimates of stress or strain in the structure.

Manuscript approved June 8, 1983.

BACKGROUND

Some previous numerical studies of simple dynamic systems are described here as examples of Hamming's motto, "The purpose of computing is insight, not numbers." [1]

Studies with Application to Shipboard Shock

Seven simple systems involving springs, rigid masses, and dynamic forces are sketched in Figure 1. Each represents some basic feature of the dynamic response of a complex structure to shock, with details stripped away. Closed-form solutions or exhaustive numerical solutions provided insight into the response of shipboard equipment to impact or shock from an underwater explosion.

For example, in Figure 1:

(a) A closed-form solution for the simple two-mass system illustrated the shock-spectrum dip and showed the importance of the effective mass of a normal mode of vibration on the response of equipment to shock delivered through ship's structure [2].

(b) Simulation of the string of five masses on an analog computer showed that the common method of determining frequencies of equipment by applying vibratory forces to the equipment itself gave incorrect results. Frequencies could be determined, however, if forces were applied to the supporting structure rather than to the equipment [3].

(c) Design charts for the three-mass system showed that under most conditions the peak responses of two items of equipment, or the responses of two normal modes of the same item, were nearly independent even though shock was delivered through a shared base. Exceptional cases (close tuning of systems having greatly-different masses) were delineated by the charts [4].

(d) The effect of simulating internal water in a structural model by filling spaces with an array of solid finite elements was investigated by calculating the passage of a shock wave through such an array placed between a pair of parallel plates [5].

(e) A mass cantilevered from a rigid base was used to investigate the effect of base rotation on the shock response of an item of equipment having a high center of gravity.

(f) The difference between the effects of yielding of the ship's structure and yielding of equipment on measurements made at the base of the equipment during underwater-explosion tests was investigated by nonlinear numerical calculations made on a three-mass model of the process [6].

(g) Design charts for a three-legged foundation intended to resist shock from two different directions were used to compare the efficiency and effectiveness of several proposed methods of designing lightweight foundations.

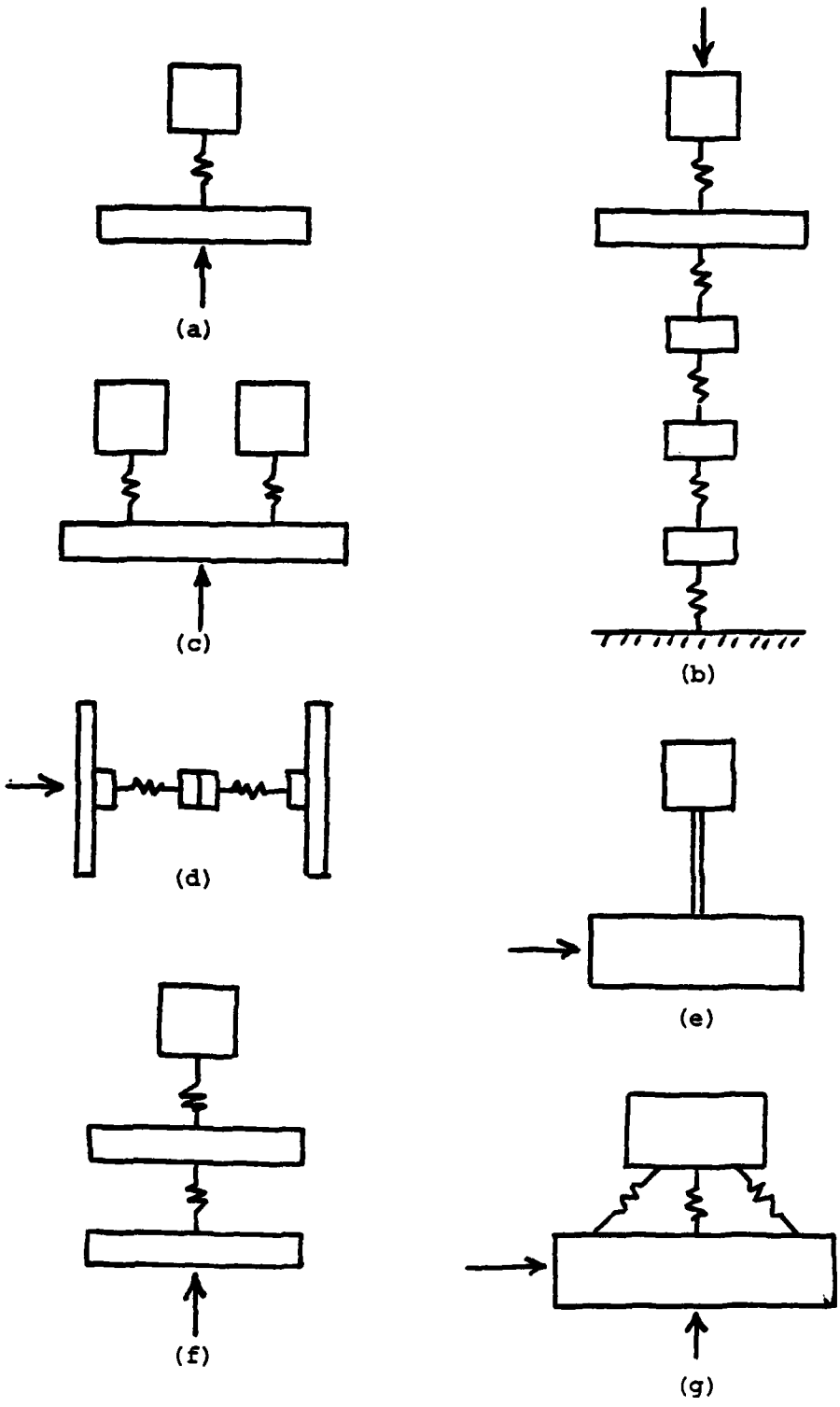

Figure 1. Simple models using springs and masses which have provided important insights for shock responses of shipboard equipment.

Response of a Square Plate to a Step Pressure

The present report builds on some results reported by Fagel in 1972 [7]. Fagel considered the case of a thin, rectangular plate with simply-supported edges subjected to a step of pressure applied to one side. He calculated time-history acceleration, velocity, and displacement at the center of the plate by superposing responses in 225 normal modes of vibration.

Fagel found that the partial modal sums for velocity and displacement converged rapidly to valid estimates of the time-history responses but that the acceleration was less cooperative. Initial acceleration for the fundamental mode was 1.62 times the ratio of pressure to mass per area for the plate. Subsequent modes had smaller initial accelerations which alternated in sign to produce a sequence whose sum converged to the proper ratio of 1.00.

In subsequent time-history superpositions of the undamped responses, however, the different frequencies of the modes caused the accelerations to combine with constantly-changing phases, leading to a divergent series for the upper bound (sum of absolute values) of the response. Nevertheless, Fagel found that the largest peak acceleration from his time-history superposition leveled off at a ratio of about 4 by the time he had included 64 symmetric modes of the plate.

A small amount of modal damping greatly decreased the number of modes needed to obtain a valid estimate of the peak acceleration at the center of the plate. The peak acceleration using nine modes was indistinguishable from the response using 225 modes if damping were set at 3 percent of critical damping for each mode, and was 15 percent lower than the 225-mode response if the damping were 1 percent. Fagel recommended that nine modes should, for practical purposes, usually be adequate for dynamic response calculations involving plates subjected to impulsive loads.

In a favorable review of Fagel's paper, [8], Hartman pointed out that the detailed calculations showed that the usual engineering approximation of applying a factor of 1.5 to the ratio of pressure to mass per area to obtain an estimate of peak acceleration of the plate was likely to be inadequate.

Plates subjected to shock waves while immersed in an acoustic fluid incur the same step of pressure as contained in Fagel's calculation, but are also damped by the acoustic resistance of the surrounding fluid. An elaboration of Fagel's calculation to include acoustic damping, a decaying shock wave, motions of supports, and a calculation of bending strain in the plate was considered worthwhile to see if his criterion for the number of modes to be used, or a similar one, could be applied to that case.

THEORY

The usual equations for a thin beam are applied to plane-strain bending of a thin plate immersed in an acoustic fluid. Plane-wave interactions with the fluid are taken for simplicity.

Equation of Motion

The differential equation

$$(EIy'')'' = 2pW - 2\rho cW(\dot{y} + \dot{b}) - m(\ddot{y} + \ddot{b}) \qquad (1)$$

represents the deflection $y(x,t)$ of a thin, rectangular plate at time t and distance x from one end of the plate. The deflection is measured relative to a moving base whose position is given by $b(t)$. Conditions are taken as uniform across the width, W, of the plate so that it bends as a beam along its length only. Both the bending stiffness EI and the mass per length m can vary along the length of the plate. The primes represent partial derivatives with respect to length x and the dots partial derivatives with respect to time t.

The plate is immersed in an acoustic fluid having plane-wave impedance ρc. A plane-wave pulse of pressure $p(t)$ is incident on one side of the plate and reflects as a plane wave, doubling the pressure applied to the plate and producing a force $2pW$ per length. It is also assumed that the plate is damped by plane waves emitted from both sides of the plate in accordance with the velocity of each area of the plate relative to the fluid. The model is a simple one chosen for illustrative purposes. Complicating influences such as curling of the plate, divergent waves in the fluid, and edge effects have been ignored.

Separation of Variables

Consider the homogeneous form of Equation 1 (no incident pressure and no base motion) and look for a solution in the form

$$y(x,t) = Y(x)\, z(t), \tag{2}$$

that is, one separable into the product of a function of position and a function of time. Substitute and write the equation as

$$\frac{(EI\ Y'')''}{m\ Y} = -\frac{\ddot{z}}{z} - \frac{2\rho c W\ \dot{z}}{m\ z}. \tag{3}$$

The left side of Equation 3 is a function of x and the right side is a function of t except for the mass per length m(x). In order to separate variables cleanly, it is necessary to require that the mass per length be constant. The right side is then independent of position on the plate, the left side is independent of time, and the only way the sides can be equal is if they are both equal to the same constant value. Write the constant as ω^2.

The left side of Equation 3 becomes

$$(EI\ Y'')'' = m\omega^2\ Y, \tag{4}$$

which is recognized as the eigenvalue equation for free vibration of a beam. If the bending stiffness EI is constant along the length, Equation 4 has the four solutions cos(ax), sin(ax), cosh(ax), and sinh(ax), with

$$a^4 = m\omega^2/(EI). \tag{5}$$

Combining the four solutions and choosing a value of a to meet four prescribed boundary conditions for a particular beam is a matter treated in standard engineering texts. As shown there, a set of different solutions $Y_n(x)$ exists, each with its own value of ω_n. Moreover, the solutions are orthogonal in the sense that

$$\int_0^L Y_k\ m\ Y_n\ dx = 0 \tag{6}$$

whenever $Y_k(x)$ and $Y_n(x)$ are solutions which correspond to different values of ω_k^2 and ω_n^2.

The value of m is shown inside the integral sign in Equation 6 because the equation applies even if m(x) is a function of position. It was only because of the second term on the right side of Equation 3 that it was necessary to require that the mass per length be independent of position along the beam.

Equation 4 shows that mY_n is proportional to $(EI\ Y_n'')''$. The orthogonality relation of Equation 6 thus implies the additional relation

$$\int_0^L Y_k (EI\ Y_n'')''\ dx = 0. \tag{7}$$

The right side of Equation 3, meanwhile, corresponds to the damped oscillator

$$\ddot{z} + 2(\rho cW/m)\ \dot{z} + \omega^2\ z = 0. \tag{8}$$

Equations 4, 6, and 7 apply to a nonuniform plate in which stiffness EI and mass per length m may both vary along the length of the plate.

Solution by Damped Normal Modes

A solution to Equation 1 which includes the incident pressure and the base motion can be obtained by writing

$$y(x,t) = \sum Y_n(x)\, z_n(t) \tag{9}$$

and taking advantage of the orthogonality of the thin-beam functions $Y_n(x)$. It is first convenient to normalize the functions by setting

$$\int_0^L Y_n m\, Y_n\, dx = 1, \tag{10}$$

where the integral is over the length of the plate. The zeroes of Equations 6 and 7 remain zero regardless of the scale factors or physical dimensions that are assigned to the functions. Making the integral be unity when the two functions are the same assigns a convenient scale factor to each function and gives it dimensions of the inverse square root of mass.

Substitute the sum of Equation 9 for $y(x,t)$ in Equation 1, multiply the equation by one of the functions, $Y_k(x)$, and integrate over the length and width of the plate. Some of the integrals vanish because of orthogonality. For the combination with k=n, the normalization produces one factor of unity and one factor

$$\int_0^L Y_n\, (EI\, Y_n'')''\, dx = \omega_n^2. \tag{11}$$

Equation 1 becomes

$$\ddot{z}_k + 2\rho c \sum \dot{z}_n\, W \int_0^L Y_k\, Y_n\, dz + \omega_k^2\, z_k = [2p - 2\rho c\, \dot{b}]\, W \int_0^L Y_k\, dx - \ddot{b} \int_0^L Y_k\, m\, dx. \tag{12}$$

Except for the second term, Equation 12 depends only on the function $Y_k(x)$ which was used as a multiplier and on the $z_k(t)$ which goes with it. The orthogonality as defined in Equation 6 eliminates cross terms in the integral of $Y_k m Y_n$ but does not generally apply to the integral of $Y_k Y_n$ which appears in the second term. Such coupling is a usual feature for modal analyses of damped structures. It comes from the mathematical theorem that, while it is usually possible to choose a set of functions to satisfy two orthogonality relations (such as Equations 6 and 7), it is hardly ever possible to satisfy three such relations. In the present case, the functions were chosen to eliminate cross terms in the mass and stiffness coefficients, leaving the damping in coupled form.

For the special case of a uniform mass per length, however, the factor m can be taken out of the integral of Equation 6 and the functions are then

also orthogonal with respect to the integral of $Y_k Y_n$. Moreover, the normalization provides a factor of 1/m so that Equation 12 becomes

$$\ddot{z}_k + 2(\rho cW/m)\,\dot{z}_k + \omega_k^2 z_k = [2pW/m - 2(\rho cW/m)\,\dot{b} - \ddot{b}]\; m \int_0^L Y_k\, dx. \tag{13}$$

Equation 13 represents an oscillator with modal damping and can be solved to show the time-history response $z_k(t)$ of the motion having modeshape $Y_k(x)$. The damping is modal (or classical) for this simplified problem only if the mass per length of the plate is uniform.

The normalization to unity indicated in Equation 10 is convenient but not necessary to the development. If the functions are chosen so that the value of the integral is other than unity, the value can be carried along with little trouble as an extra factor; its inverse eventually appears as a factor on the right side of Equations 12 or 13.

Note particularly that the value of the integral of Equation 10 for unnormalized functions has no physical significance. It is simply a scale factor resulting from inappropriate normalization, with a value which depends on the arbitrary scale factors applied to the orthogonal functions. In some treatments it is incorrectly identified as an "effective mass".

A proper interpretation of effective modal mass is easily obtained if Equation 10 is normalized to a dimensionless unity and the functions $Y_n(x)$ are interpreted as having dimensions of the inverse square root of mass. The integral of $Y_k m$ which appears on the right side of Equations 12 and 13 (commonly called the participation factor) then has dimensions of the square root of mass, and the square of the participation factor is, indeed, the effective modal mass which provides a reaction force against the base motion when Mode k is accelerated.

Pressure Pulse from a Shock Wave

The incident pressure pulse p(t) was taken as

$$p = p_0 e^{-t/\Theta} \tag{14}$$

to represent the shock wave from an underwater explosion. At time t=0 the pressure jumps abruptly to a peak value of p_0 and thereafter decays exponentially with time constant Θ. Water is customarily treated as an acoustic medium over the range of pressures of interest to fluid-structure interactions although nonlinear processes are important to the initial formation of the shock wave.

Flat-Plate Base Motion

If a plate is not connected to a base and undergoes no bending, Equation 1 becomes

$$m \ddot{y} = 2pW - 2\rho cW \dot{y}. \tag{15}$$

This equation was used to generate base motions b(t) for some of the calculations. The presumption was that the plate of interest was mounted to a larger and heavier plate on which the pressure pulse acted.

If the pressure pulse is a shock wave, the flat plate begins moving with an abrupt acceleration of $2p_0W/m$ at time zero and reaches a peak velocity of $p(t)/(\rho c)$ at time t. A closed-form solution for the motion is easily obtained.

Sphere Base Motion

The velocity u(t) of a rigid sphere of radius r struck by a plane shock wave with pressure p(t) in an acoustic fluid of density ρ and sound speed c satisfies the differential equation

$$M\ddot{u} + 2(M+F/2)\,(c/r)\dot{u} + 2(M+F/2)\,(c/r)^2 u = 3F(c/r)^2 p/(\rho c). \tag{16}$$

where M is mass of the sphere and

$$F = (4/3)\pi r^3 \rho \tag{17}$$

is the mass of an equal volume of fluid. A closed-form solution is available [9] for the case in which p(t) is a shock wave.

The reponse of a sphere to a shock wave was used as a base motion for some of the calculations. As for the case of the flat-plate base motion, it was assumed that the plate of interest was supported from a heavy sphere which was subjected to the incident shock wave. The flat-plate motion began with an abrupt step to peak acceleration, while the onset of acceleration is more gradual for the sphere.

RESULTS

Computer programs were written to find modeshapes and frequencies for thin cantilevered beams, to calculate time-history responses of the modes to a shock wave and a variety of base motions, and to superpose bending strains from various combinations of modes.

Parameters Used in Calculations

For convenience, calculations were done in dimensional form with dimensions fitted to some available data from small-scale tests [9]. Calculations and data from the tests could then be used directly to assess the accuracy and realism of some of the intermediate steps in the analysis.

Plates were of steel, 254 mm long, 152 mm wide, and either 3.3 or 9.3 mm thick, supported from one end as cantilevers. The incident shock wave had a peak pressure of 6.96 MPa and decayed exponentially from the peak with a time constant of 0.425 ms. Base motions were taken as produced by the action of the shock wave on a flat plate or a sphere having a mass of 272 kg, with a surface area of $0.395 m^2$ for the plate and a radius of 162 mm for the sphere. Some of the calculations used plates or spheres having different characteristics to explore the effect of variations.

Results are shown as values of bending strain at the surface of the plate. Stress is strain multiplied by the elastic modulus of 207 GPa which was used in the calculations.

Frequencies and Modeshapes

Table 1 lists the first 30 normal-mode frequencies of a steel cantilever beam 254 mm long and 9.3 mm thick, as determined by direct fitting of the thin-beam formula

$$Y_n = [\cosh(a_n x) - \cos(a_n x)] - \sigma_n[\sinh(a_n x) - \sin(a_n x)] \qquad (18)$$

to conditions of a fixed end at x=0 and a free end at x=254 mm. Calculations were done in double precision on the ASC (Advanced Scientific Computer) at the Naval Research Laboratory. Procedures and notations were taken from the textbook by Mario Paz [10]. It was necessary to discount the values shown for the first five modes of a cantilever in Table 20.4 of the textbook, which appeared to be in error.

The column labeled "SIGMA(N)" in Table 1 is the value of σ_n needed in Equation 18. The column "MODE CONST" is the ratio of the integral of $Y_n(x)$ to the integral of $Y_n^2(x)$ over the length of the beam. This is the factor needed on the right side of Equation 13 because the modeshapes are not normalized.

Strain at the surface of the beam is given by

$$\varepsilon = \sum (H/2)\, Y_n'' \, z_n \qquad (19)$$

where H is thickness of the beam, $Y_n''(x)$ is the curvature (second derivative) obtained from the modeshapes above, and $z_n(t)$ is time-history response of the mode.

TABLE 1 - THIRTY MODES OF A CANTILEVER

MODE	FREQ(HZ)	MODE CONST	SIGMA(N)
1	0.11960D 03	0.78299D 00	0.73410D 00
2	0.74951D 03	0.43393D 00	0.10185D 01
3	0.20987D 04	0.25443D 00	0.99922D 00
4	0.41125D 04	0.18191D 00	0.10000D 01
5	0.67983D 04	0.14148D 00	0.10000D 01
6	0.10155D 05	0.11575D 00	0.10000D 01
7	0.14184D 05	0.97941D-01	0.10000D 01
8	0.18884D 05	0.84883D-01	0.10000D 01
9	0.24255D 05	0.74896D-01	0.10000D 01
10	0.30298D 05	0.67013D-01	0.10000D 01
11	0.37013D 05	0.60512D-01	0.10000D 01
12	0.44398D 05	0.67468D-01	0.10000D 01
13	0.52456D 05	0.25465D-01	0.10000D 01
14	0.61184D 05	0.47157D-01	0.10000D 01
15	0.70584D 05	0.43905D-01	0.10000D 01
16	0.80656D 05	0.41072D-01	0.10000D 01
17	0.91399D 05	0.38583D-01	0.10000D 01
18	0.10281D 06	0.36378D-01	0.10000D 01
19	0.11490D 06	0.34412D-01	0.10000D 01
20	0.12766D 06	0.32647D-01	0.10000D 01
21	0.14108D 06	0.31055D-01	0.10000D 01
22	0.15518D 06	0.29610D-01	0.10000D 01
23	0.16996D 06	0.28294D-01	0.10000D 01
24	0.18540D 06	0.27090D-01	0.10000D 01
25	0.20151D 06	0.25984D-01	0.10000D 01
26	0.21830D 06	0.24965D-01	0.10000D 01
27	0.23576D 06	0.24023D-01	0.10000D 01
28	0.25388D 06	0.23150D-01	0.10000D 01
29	0.27268D 06	0.22338D-01	0.10000D 01
30	0.29216D 06	0.21580D-01	0.10000D 01

Approximate Modeshapes

The functions

$$Y_n = N[\sin(a_n x) - \cos(a_n x) + e^{-a_n x} - (-1)^n e^{-a_n (1-x)}], \quad (20)$$

with

$$a_n = (n - \tfrac{1}{2})\pi/L, \quad (21)$$

provide end conditions

$$Y_n(0) = -N (-1)^n e^{-a_n L}, \quad (22)$$

$$Y_n'(0) = -N a_n (-1)^n e^{-a_n L}, \quad (23)$$

$$Y_n''(L) = N a_n^2 e^{-a_n L}, \quad (24)$$

$$Y_n'''(L) = -N a_n^3 e^{-a_n L}. \quad (25)$$

They form an orthogonal set with

$$\int_0^L Y_n \, m \, Y_n \, dx = 1 - 2(-1)^n e^{-a_n L} - e^{-2a_n L}/(a_n L) \quad (26)$$

if N is chosen to satisfy

$$N^2 L m = 1. \quad (27)$$

They also provide

$$m \int_0^L Y_n \, dx = 2/(N a_n L) - [1 - (-1)^n] e^{-a_n L}/(N a_n L). \quad (28)$$

The factors $e^{-a_n L}$ which appear in the preceding equations decrease rapidly with increasing n and are smaller than 0.00002 for n=4 or larger. If the exponential terms are neglected in Equations 22 through 28, the functions can be used as a set of orthonormal modes for a thin beam which satisfy the end conditions for a cantilever. They are, in fact, excellent approximations from the fourth mode onward. The important and convenient

features of the approximations are the closed-form representations for the participation factor

$$m \int_0^L Y_n \, dx = 2/[(n - \tfrac{1}{2})\pi N] \tag{29}$$

and the frequency

$$\omega_n = (EI/m)^{1/2} [(n - \tfrac{1}{2})\pi]^2/L^2 \, . \tag{30}$$

The participation factor for the fourth mode from Equation 29 is 0.18189, compared to the value of 0.18191 as the mode constant for the exact solution listed in Table 1. Differences are smaller for higher modes.

Initial Acceleration

With initial conditions $z_n(0) = \dot{z}(0) = 0$, Equation 13 shows an initial acceleration of

$$\ddot{z}_n(0) = \ddot{g}(0)\, m \int_0^L Y_n\, dx, \tag{31}$$

where

$$\ddot{g} = 2pW/m - 2(\rho cW/m)\,\dot{b} - \ddot{b} \tag{32}$$

represents the combined inputs from the incident pressure and the base motion.

The initial acceleration at any point on the beam is

$$\ddot{y}(x,0) = \ddot{g}(0) \sum Y_n(x)\, m \int_0^L Y_n\, dx. \tag{33}$$

If the approximate mode functions are used, the modeshape at the tip (for example) is

$$Y_n(L) = -2\, N\, (-1)^n \tag{34}$$

and the acceleration there is given by

$$\ddot{y}(L,0) = \ddot{g}(0) \sum -4\, (-1)^n / [n - \tfrac{1}{2}\pi]. \tag{35}$$

The sum in Equation 35 converges to a value of 2, but half of that value comes from differences of 0.98050, 0.01903, 0.00044, and 0.00003 between the approximations of Equations 29 and 34 and the exact solution from fitting Equation 18 for the first four terms in the series.

Convergence of the series for the first 30 modes is illustrated in Table 2. The convergence is slow - seven modes are needed to come within 10 percent of the correct factor of unity, thirteen modes for 5-percent accuracy, and 32 modes for 2-percent accuracy.

TABLE 2 - CONVERGENCE OF MODAL SERIES

FOR A THIN CANTILEVERED BEAM

Mode Number	Tip Acceleration Factor	Tip Acceleration Sum	Upper Bounds for Light Damping: Acceleration at Tip	Velocity at Tip	Deflection at Tip	Strain at Base
1	1.566 a	1.566	1.566	0.445	0.1267	0.445
2	-0.868 a	0.698	2.434	0.485	0.1285	0.485
3	0.509 b	1.207	2.943	0.493	0.1286	0.493
4	-0.364	0.843	3.307	0.496	c	0.496
5	0.283	1.126	3.536	0.498		0.498
6	-0.231	0.895	3.767	0.498		0.498
7	0.196	1.090	3.963	0.499		0.499
8	-0.170	0.921	4.133	0.499		0.499
9	0.150	1.071	4.283	0.499		0.499
10	-0.134	0.936	4.417	0.499		0.499
11	0.121	1.058	4.538	0.500		0.500
12	-0.111	0.947	4.649	c		c
13	0.102	1.049	4.751			
14	-0.094	0.955	4.845			
15	0.088	1.042	4.933			
16	-0.082	0.960	5.015			
17	0.077	1.037	5.092			
18	-0.073	0.965	5.165			
19	0.069	1.033	5.234			
20	-0.065	0.968	5.299			
21	0.062	1.030	5.361			
22	-0.059	0.971	5.420			
23	0.057	1.028	5.477			
24	-0.054	0.973	5.531			
25	0.052	1.025	5.583			
26	-0.050	0.976	5.633			
27	0.048	1.024	5.681			
28	-0.046	0.977	5.727			
29	0.045	1.022	5.772			
30	-0.043	0.980	5.815			

a - Exact solutions used for Modes 1 and 2.
b - Approximation (see text) agrees with exact solution through all significant figures shown for Modes 3 and subsequent.
c - No subsequent change to accuracy shown.

Peak Responses of Heavily-Damped Modes

A peak (maximum or minimum) velocity which occurs at time t_n' corresponds to a vanishing acceleration,

$$\ddot{z}(t_n') = 0 \tag{36}$$

so that Equation 13 becomes

$$2(\rho cW/m)\, \dot{z}_n(t_n') + \omega_n^2\, z_n(t_n') = \ddot{g}(t_n')\, m \int_0^L Y_n\, dx. \tag{37}$$

If the damping rate $\rho cW/m$ is large compared to the frequency ω_n, the term in ω_n^2 can be neglected to show that the peak velocity is proportional to the participation factor.

If Equation 13 is integrated once, peak deflections occur when

$$\dot{z}_n(t_n'') = 0 \tag{38}$$

and, for heavy damping, are given approximately by

$$z_n(t_n'') = [m/(2\rho cW)]\, \dot{g}(t'')\, m \int_0^L Y_n\, dx. \tag{39}$$

The plane-wave damping rate is the same for each mode. The peak velocities for all of the damping-controlled modes thus occur simultaneously at times $t_n' = t'$, and the peak displacements all occur at $t_n'' = t''$. Determining the peak values by superposing the peaks from each mode leads to a sum which converges in the same slow fashion as the sum from the initial acceleration as shown in Table 2.

Curvature of the approximate modeshape at the base (for example) of the cantilever is

$$Y_n''(0) = 2\, N\, a_n^2 \tag{40}$$

and the peak strain there is given by

$$\varepsilon(t'') = (H/2)\, [m/(2\rho cW)]\, \dot{g}(t'') \sum 4\, (n - \tfrac{1}{2})\pi. \tag{41}$$

The sum of Equation 41 diverges by showing an accumulation of larger and larger values of strain from successive modes.

The oscillator of Equation 13 is overdamped whenever $\rho cW/m$ is larger than ω_n. For a steel plate 9.3 mm thick immersed in sea water, $\rho cW/m$ has the value 21,790 radians per second, so that modes having frequencies up to 3468 Hz will respond as overdamped oscillators. Modes 1, 2, and 3, as listed in Table 1 with frequencies 120, 750, and 2099 Hz, are overdamped for this plate. A plate with thickness 3.3 mm has damping rate 61,347 rad/s, with overdamped modes up to 9764 Hz. This range covers the first six modes for the thinner plate.

Upper Bounds for Peak Responses of Lightly-Damped Modes

If the input $\ddot{g}(t)$ includes a sudden change at time zero (as from the step pressure at the leading edge of a shock wave, for example), the lightly-damped (high-frequency) modes will respond to the step with oscillations at nearly their undamped frequencies and will reach peak values of velocity, acceleration, and deflection at about one-quarter, one-half, and one period after the step. The peaks recur at half-period intervals, decreasing in magnitude as a result of the light damping. An upper-bound to the time-history response from a superposition of modal responses is given by the sum of the absolute values of the peaks for the modes on the supposition that it is possible (although improbable) that all of the peak values might occur in the same direction at some time before their amplitudes had been appreciably reduced by the damping.

A step input which produces an initial acceleration $\ddot{z}_n(0)$ causes lightly-damped modes to begin vibrating with initial amplitudes of $\dot{z}_n(0)/\omega_n$ for velocity and $z_n(0)/\omega_n^2$ for displacement. A sum over absolute values, using the approximate modeshapes, gives upper-bounds

$$\ddot{y}(L,t) < \ddot{g}(0) \sum 4/[(n - 1/2)\pi], \tag{42}$$

$$\dot{y}(L,t) < \ddot{g}(0)\, L^2\, [m/EI)]\, 1/2 \sum 4/[(n - 1/2)\pi]^3, \tag{43}$$

$$y(L,t) < \ddot{g}(0)\, L^4\, [m/EI)] \sum 4/[(n - 1/2)\pi]^5, \tag{44}$$

for acceleration, velocity, and deflection at the tip, and

$$\varepsilon(0,t) < \ddot{g}(0)\, (H/2)\, L^2\, [m/(EI)] \sum 4/[(n - 1/2)\pi]^3 \tag{45}$$

for strain at the base. The oscillations represent motions relative to the base of the cantilever and take place about an equilibrium deformation established by the net pressure on the plate and the acceleration of its base.

Values of the partial sums from Equations 42 through 45 are listed in Table 2 for the first 30 modes of the beam. The upper-bound for the acceleration at the tip increases steadily, but at a decreasing rate, as additional modes are added to the sum. If the sum were terminated after the 30 modes shown, the smallest peak acceleration in the next block of 30 modes (from n=31 to n=60) block would have a factor $4/(59.5\,\pi)$ and the sum of the 30 terms in the block would be larger than $30[4/(60\,\pi)] = 0.637$. The sum ought to be extended to n=60 to include this significant contribution. But the sum would still not be complete, since extending it to n=120 would provide another block of 60 terms accumulating to more than 0.637, and so on.

The influence of the frequency makes the partial sums for velocity, deflection, and strain converge promptly. The first two modes provide a peak strain which is a 3 percent low; the first three modes account for 99 percent of the upper-bound sum of the strains over all the modes. The first mode alone accounts for 99 percent of the upper-bound on the deflection at the tip.

The approximate calculations described here indicate that the peak strains in the beam, calculated and superposed mode-by-mode, are likely to begin as a divergent series for the low-frequency, heavily-damped modes. As the effects of stiffness become predominant for the higher-frequency modes, the superposed strains should converge rapidly to a final value. Detailed numerical calculations are needed to verify the expected increase, turnaround, and eventual convergence of the strains with increasing numbers of modes.

Time Histories and Superposition

Equation 13 for the response of each mode was solved using Runge-Kutta fourth-order integration with short time steps. Results were converted to strains at particular locations using the exact modeshapes (Equations 18 and 19) and the strains were added up mode-by-mode to determine time-history bending responses. Partial sums over various numbers of modes were displayed as a function of time and inspected to determine rate of convergence in general and the number of modes needed to approach final values in particular cases.

Figures 2 through 5 show partial sums for time-history strains near the base of two plates of different thicknesses when they are struck by a shock wave with peak pressure about 7 MPa and time constant about 0.4 ms. A sum over 8 modes is needed to obtain substantial convergence for the thicker plate (Figure 2), with little change thereafter (Figure 3). The thinner plate needs 20 modes (Figure 4) to arrive substantially at its final values of strain (Figure 5).

Similar results were obtained for other locations on the plates and for other combinations of inputs. Strains on the thicker plate converged in fewer than 12 modes at two locations farther from the base (Figures 6 and 7). The convergence continued when the input consisted of the flat-plate base motion followed, 0.1 ms later, by the shock wave (Figure 8 at one location, other locations not illustrated) or the base motion from the sphere followed by the shock wave (not illustrated).

Strains in the thinner plate from the shockwave alone had converged by 20 modes (Figures 9 and 10), as was the case when the input consisted of the base motion from the flat plate or the sphere followed by the shock wave (Figures 11 and 12).

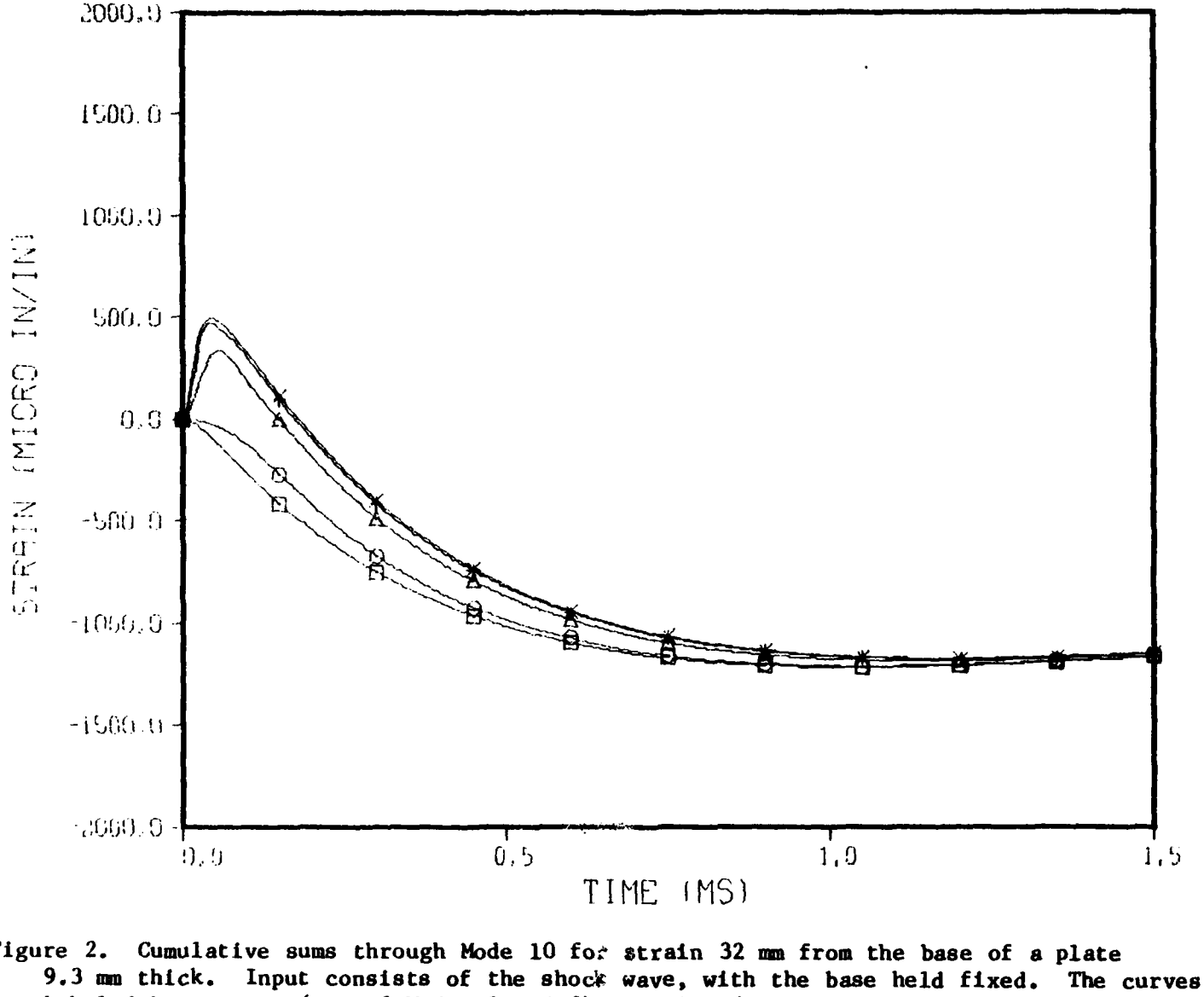

Figure 2. Cumulative sums through Mode 10 for strain 32 mm from the base of a plate 9.3 mm thick. Input consists of the shock wave, with the base held fixed. The curves are labeled by squares (sum of Modes 1 and 2), circles (sum of Modes 1 through 4), triangles (1 through 6), plus signs (1 through 8), and letters X (1 through 10). Markers are in the same sequence for subsequent figures.

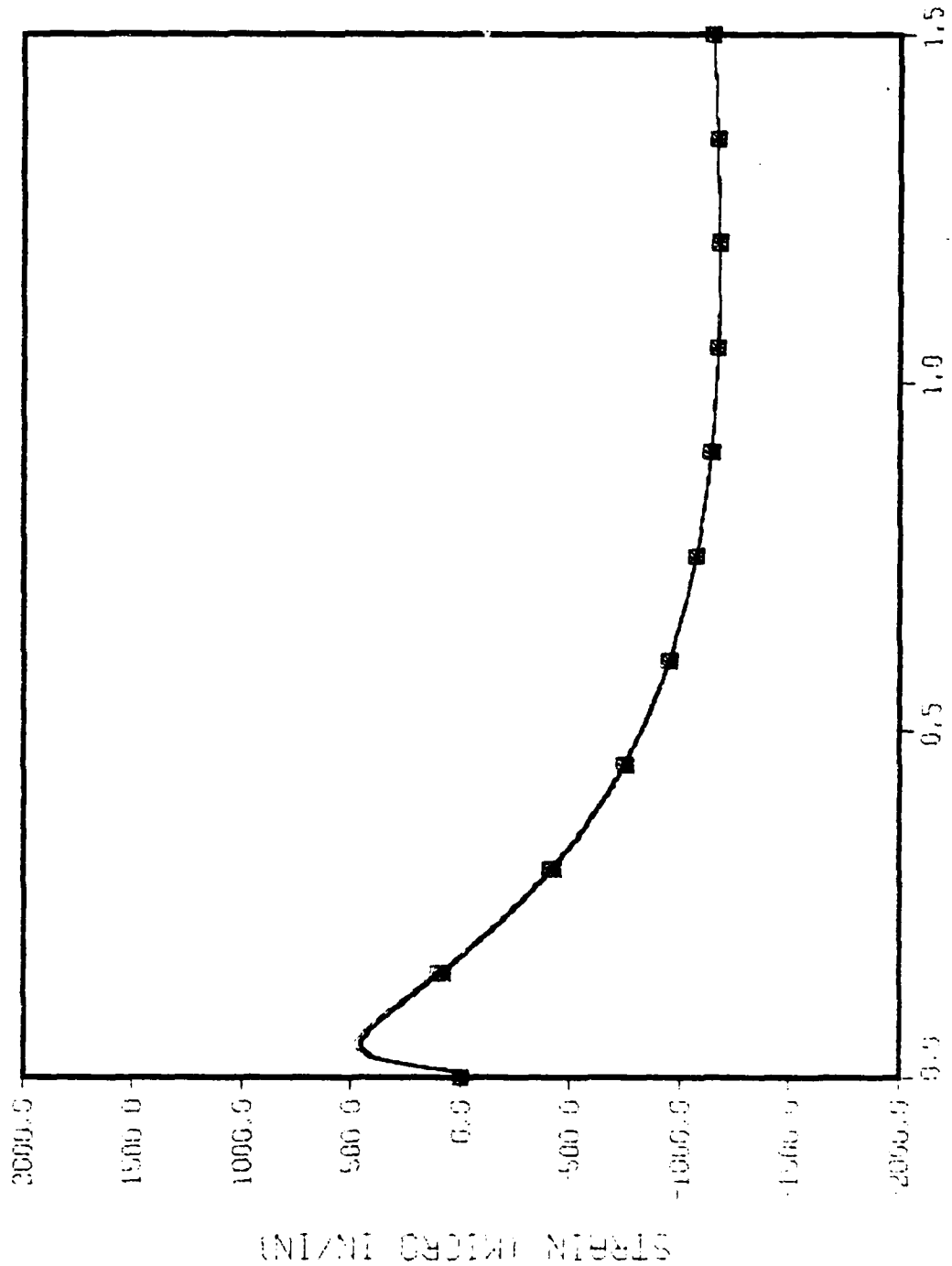

Figure 3. Continuing Figure 2, with cumulative sums through Modes 12, 14, 16, 18, and 20.

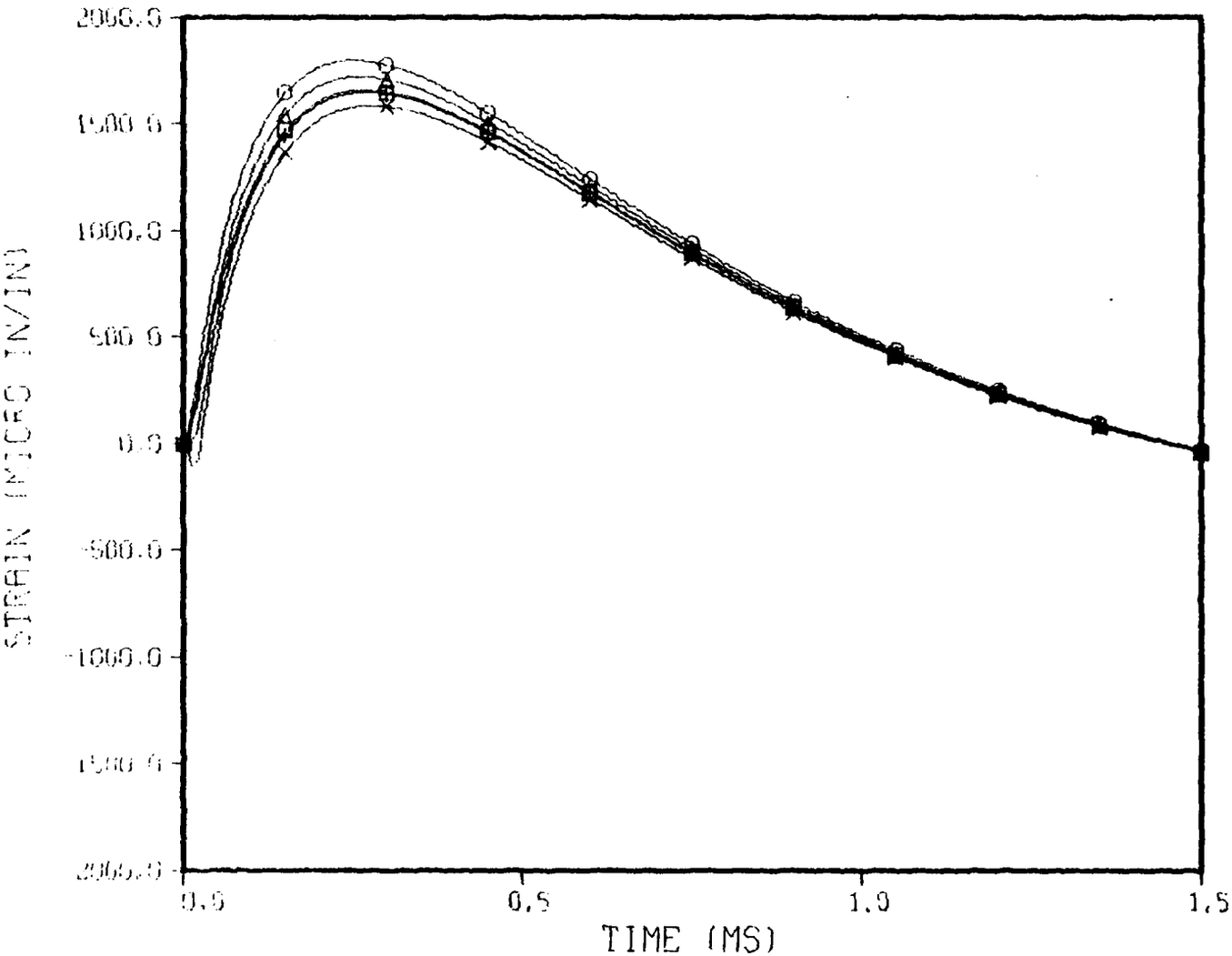

Figure 4. Cumulative sums through Modes 8, 10, 12, 14, and 16 for strain 32 mm from the base of a plate 3.3 mm thick. Input consists of the shock wave, with the base held fixed.

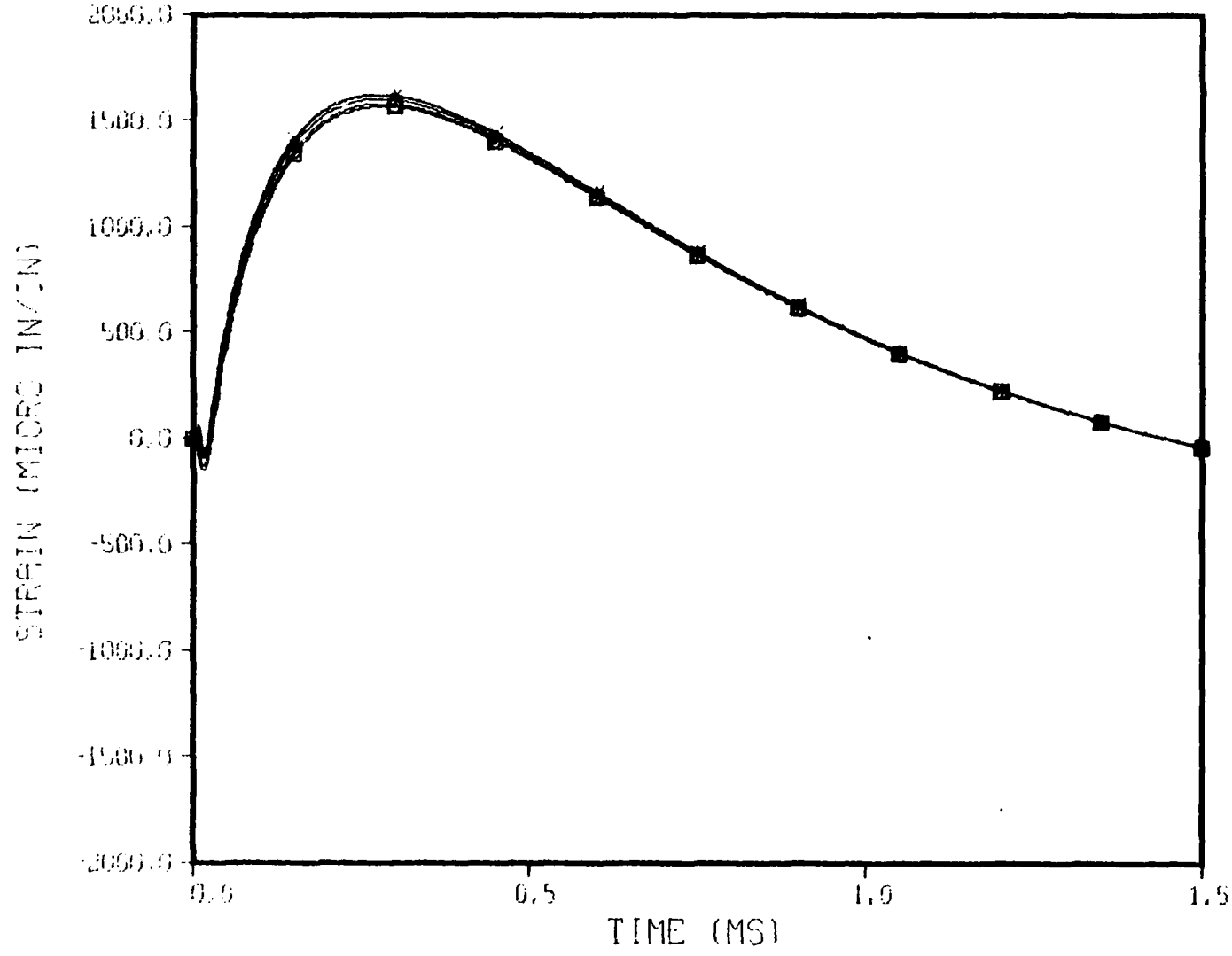

Figure 5. Continuing Figure 4, with cumulative sums through Modes 18, 20, 22, 24, and 26.

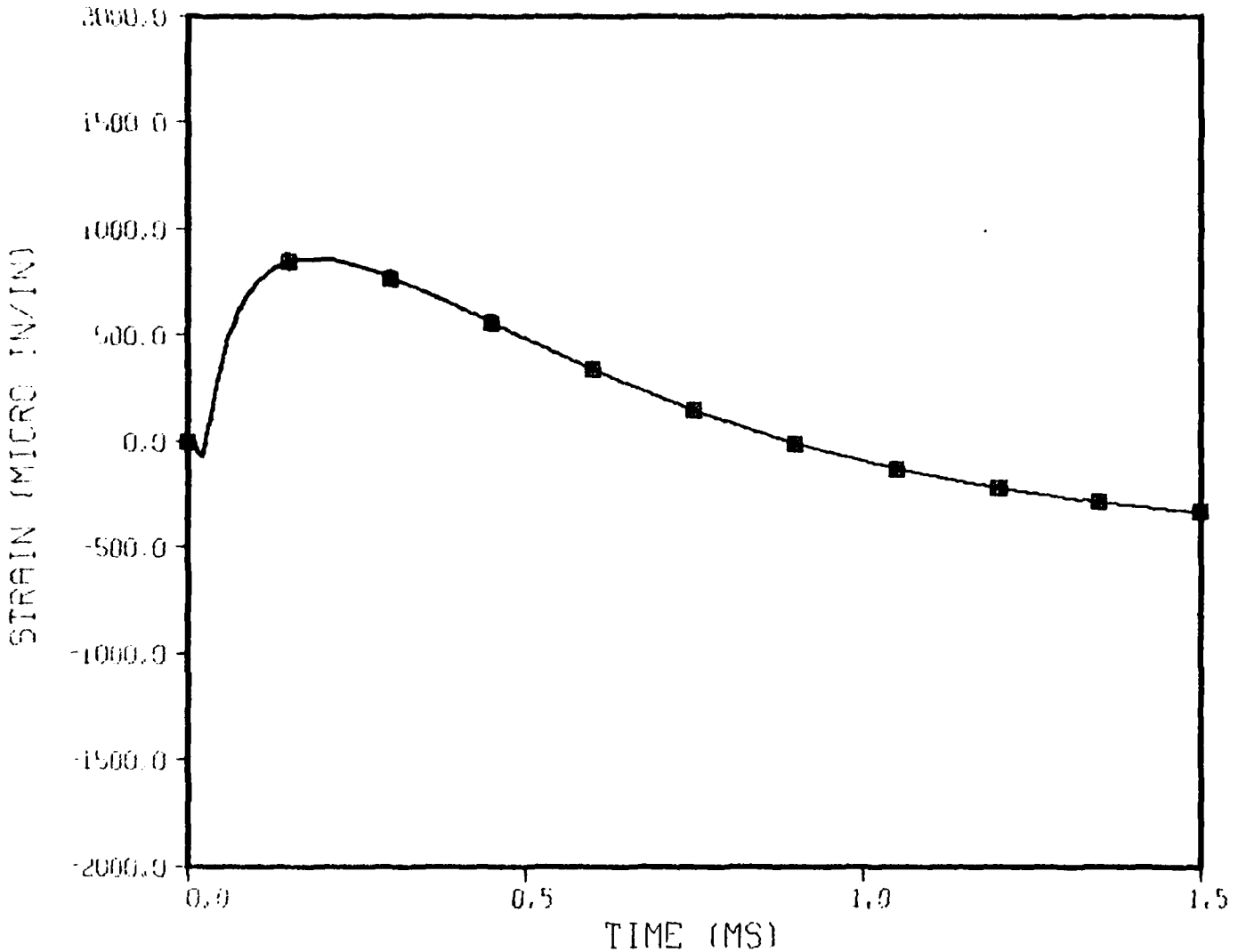

Figure 6. Cumulative sums through Modes 12, 14, 16, 18, and 20 for strain 57 mm from the base of a plate 9.3 mm thick. Input consists of the shock wave at time zero.

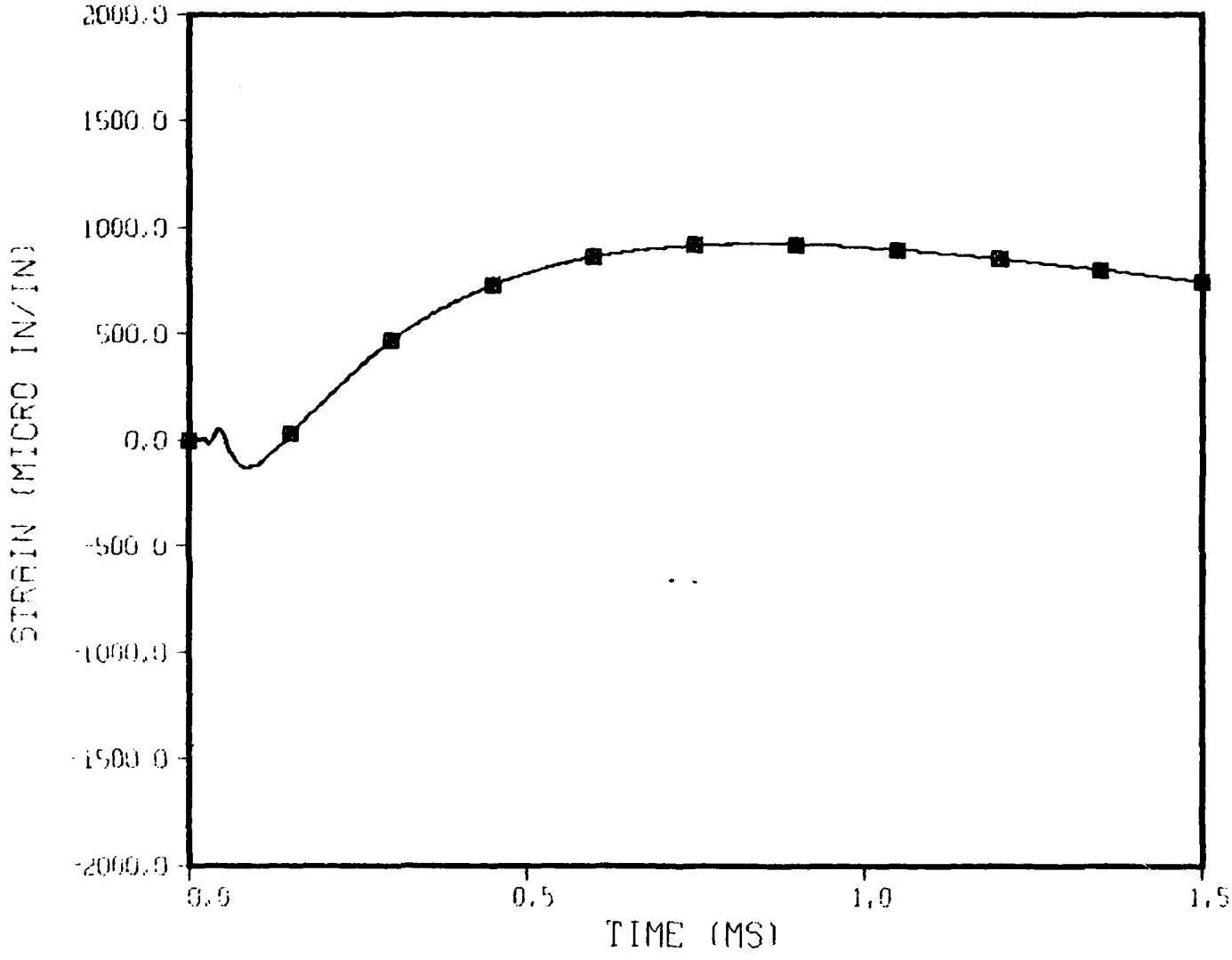

Figure 7. Same as Figure 6 but showing strain 121 mm from the base.

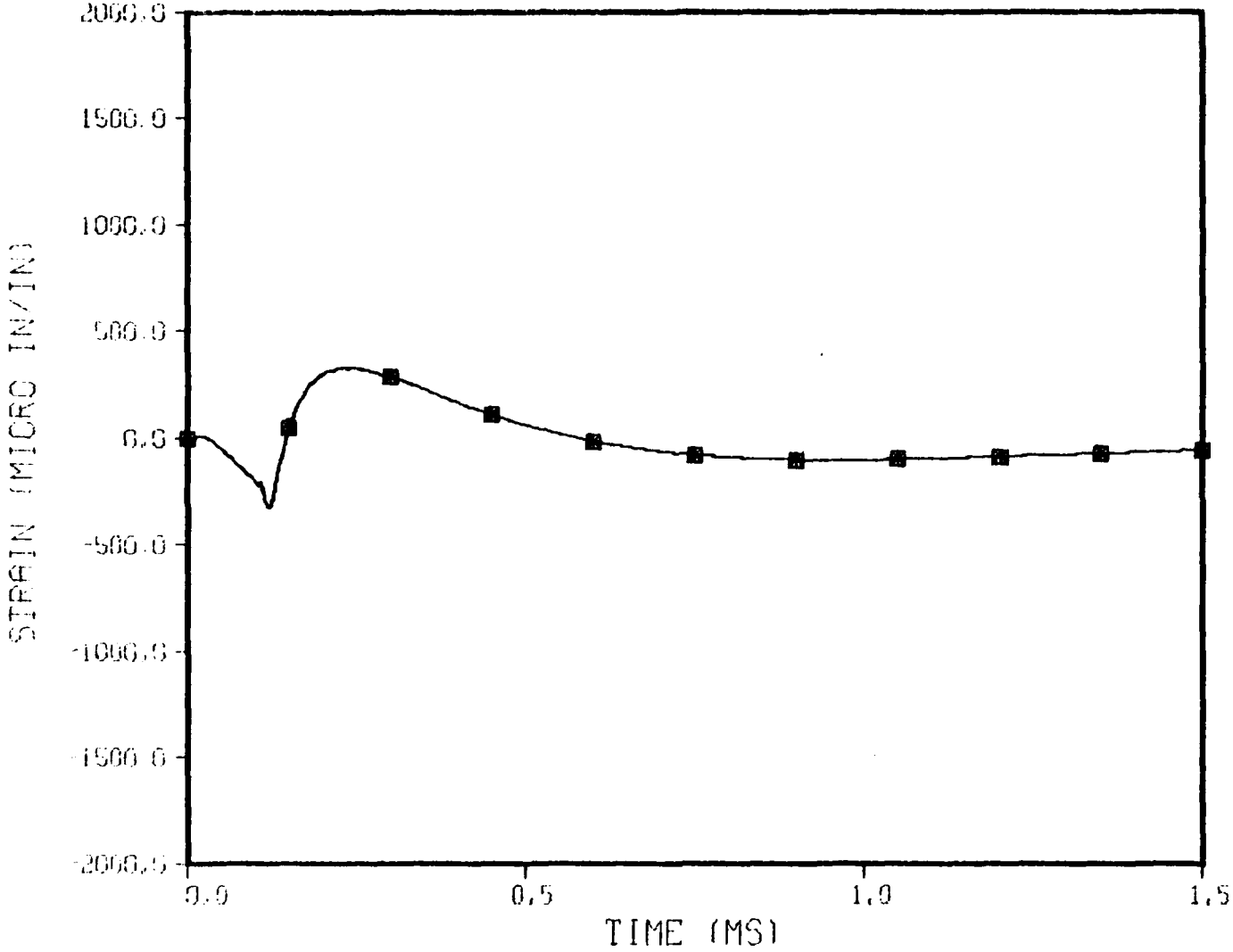

Figure 8. Same as Figure 6 but input consists of shock wave arriving at 0.1 ms, preceded by a base motion consisting of the response of a heavy flat plate to the shock wave beginning at time zero.

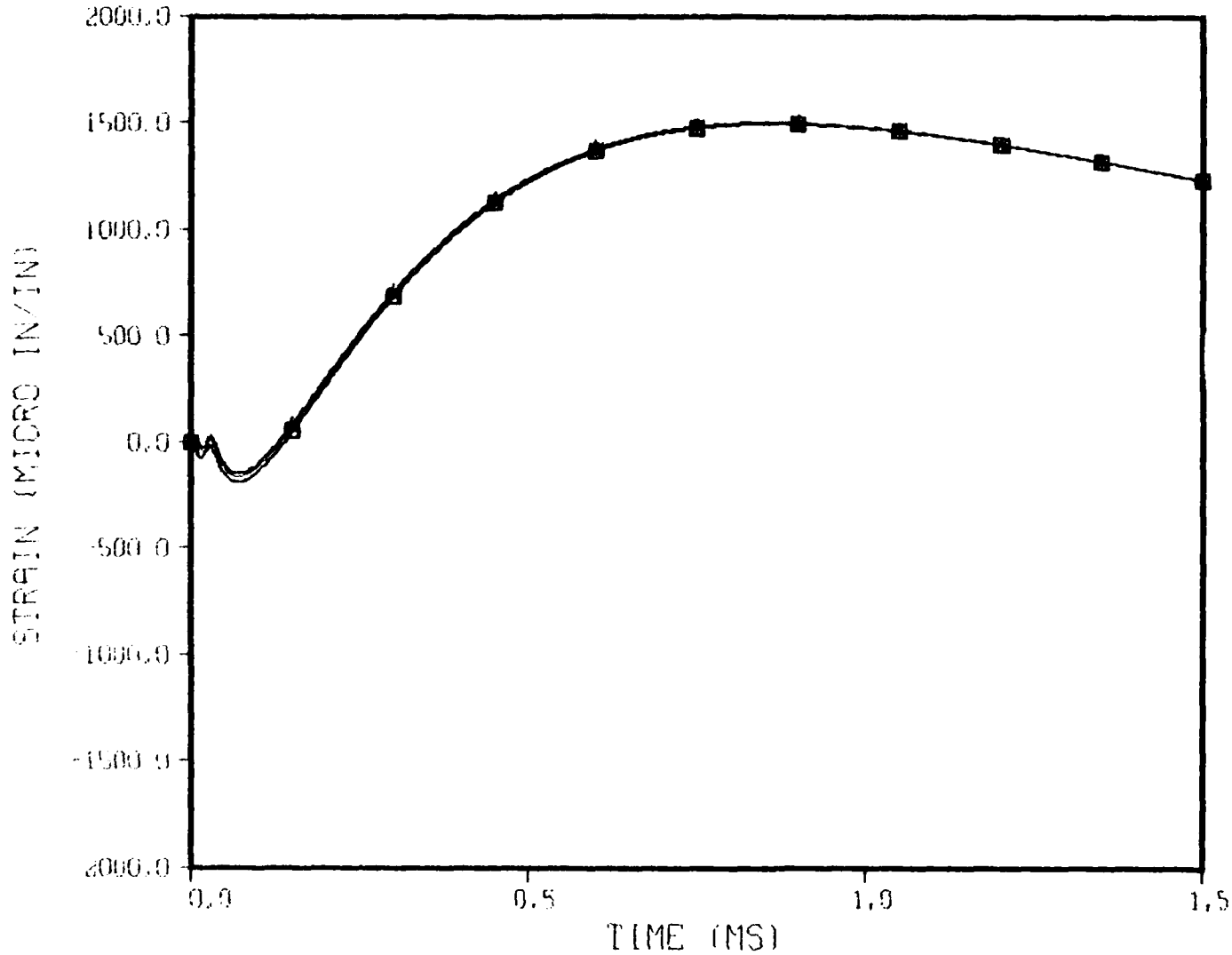

Figure 9. Cumulative sums through Modes 18, 20, 22, 24, and 26 for strain 57 mm from the base of a plate 3.3 mm thick. Input consists of the shock wave at time zero.

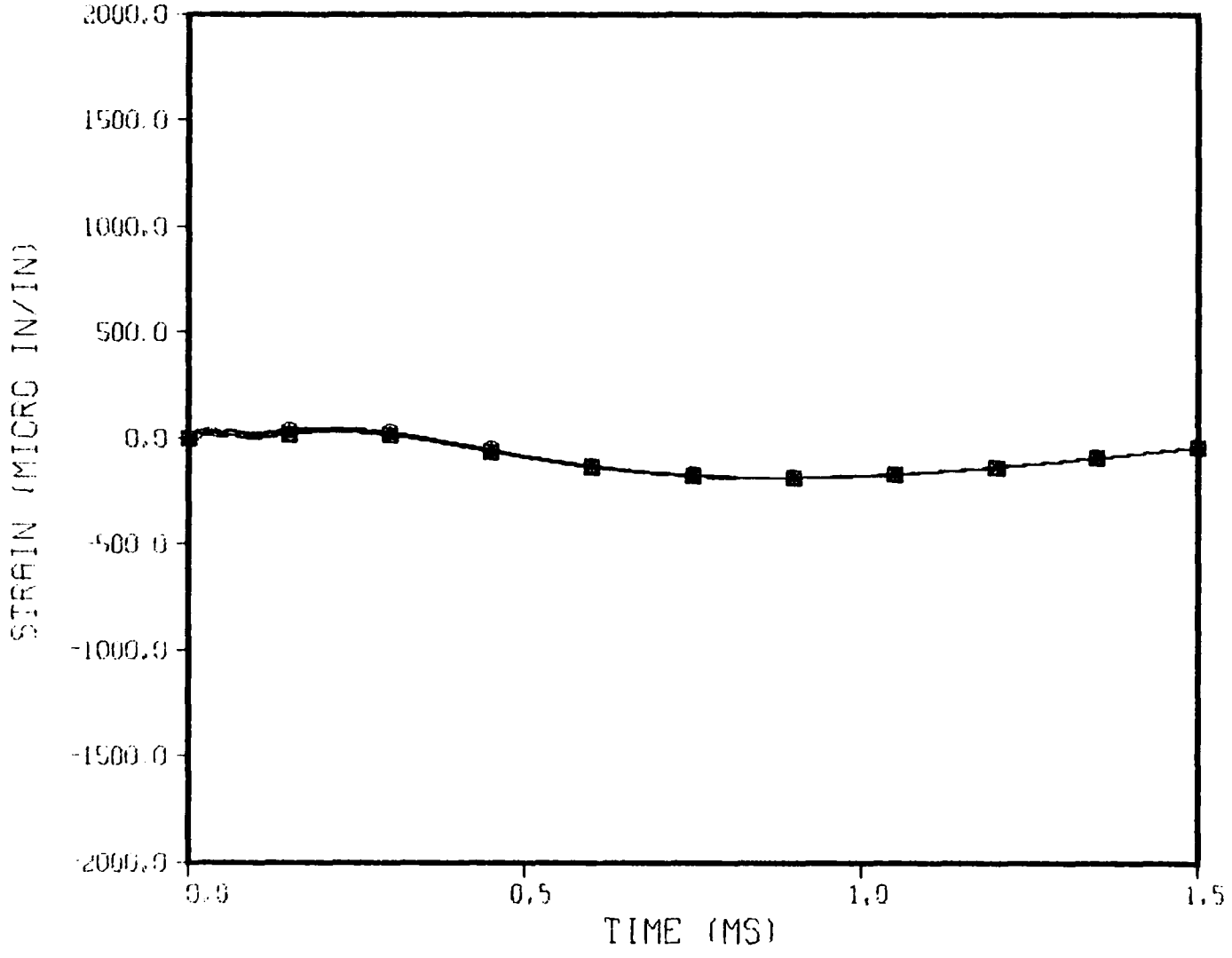

Figure 10. Same as Figure 9 but showing strain 121 mm from the base.

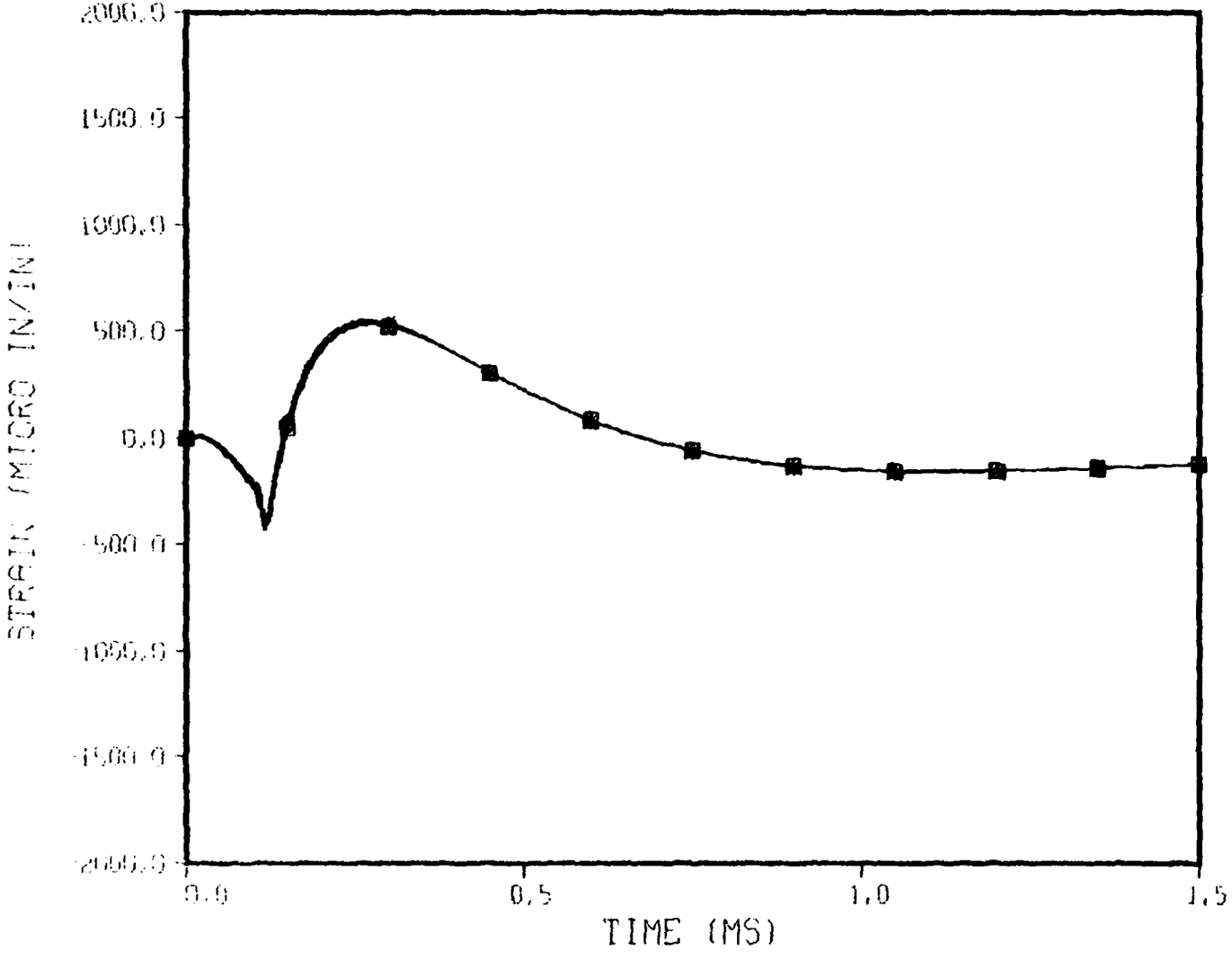

Figure 11. Same as Figure 9 but for strain 32 mm from the base and for combined inputs. Input consisted of base motion from the response of a heavy flat plate to the shock wave at time zero, followed by the shock wave at time 0.1 ms.

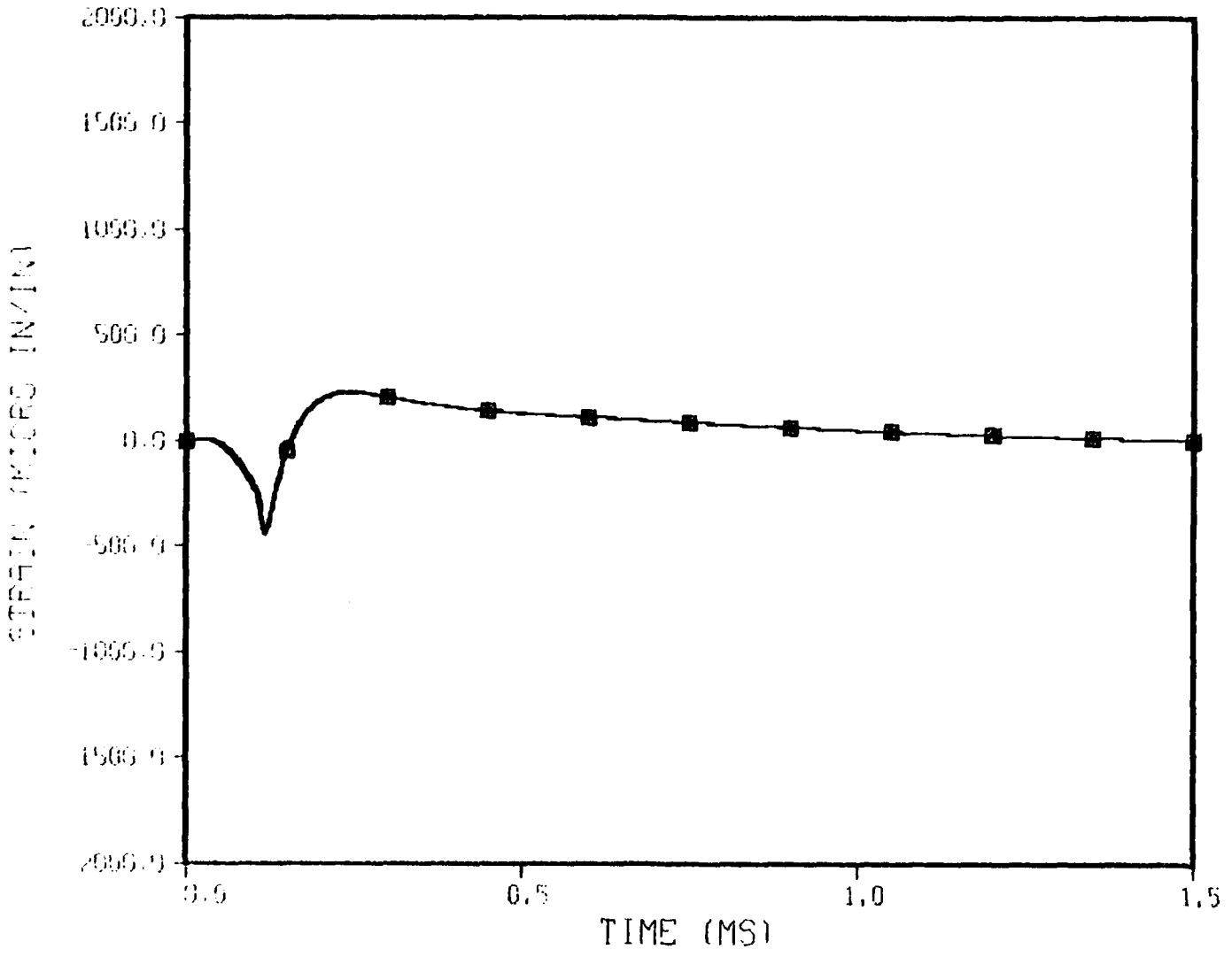

Figure 12. Same as Figure 11 but with base motion from a heavy sphere. For this calculation the sphere was taken to have a mass of 118 kg and a radius of 162 mm.

DISCUSSION

The calculations show that the number of modes needed to produce convergence of time-history strains to final values depends on the damping. From 8 to 20 modes were needed for the examples used here. The requirement to analyze plates for modes having high frequencies and short wavelengths means that the plates must be represented by modal formulas which are adequate in that range, by high-order finite elements, or by a large number of small finite elements if strains are to be determined properly.

Damping

Damping relative to critical is given by $\rho cW/(m\omega)$ for the calculations made here (plane-wave damping from the in-vacuo modes of a plate immersed in an acoustic fluid). It ranged from 230 times critical for the first mode (42 Hz) of a steel plate 3.3 mm thick immersed in sea water to 1 percent of critical for the thirtieth mode (292 kHz) of a plate 9.3 mm thick.

The numerical results showed that 8 modes were needed to converge to nearly the final values of strain for the thicker plate, as indicated in Figure 2, for example. The eighth mode had a frequency of 19 kHz with damping 18 percent of critical. A corresponding approach toward convergence for the thinner plate required 20 modes, as shown in Figure 5. There the twentieth mode had a frequency of 45 kHz and damping 22 percent of critical.

As described earlier, the strains for the heavily-damped, low-frequency modes begin as a divergent series. Under the influence of a shock wave or a base motion, these modes tend to have displacements proportional to the relative displacement between the surrounding water and the base. The curvature of the modes, which establishes the strain at the surface of the plates, is approximately proportional to frequency times deflection and increases with increasing mode frequency.

Lightly-damped modes, however, tend to have oscillatory deflections with amplitudes which are inversely proportional to the square of the frequency. Strains from these modes decrease with increasing frequency, so that the sum of the strains approaches a limiting value. Calculations for strain need to be carried through the regime of the overdamped modes and into the range of the lightly-damped modes before convergence occurs. For the two thicknesses of plate considered here, this seemed to involve including modes with dampings down to 20 percent or so of critical damping.

Adequacy of Structural Representation

Thin-beam formulas, as used in the present calculations, are generally considered adequate for beams whose thickness is less than 1/10 of the distance between nodes. On this criterion, the frequencies and modeshapes as calculated were inaccurate from the third mode onward for the thicker plate, and from the eighth mode onward for the thinner plate. At the modes producing convergence (the eighth for plates 9.3 mm thick, or the twentieth for plates 3.3 mm thick, both plates 254 mm long), the distance between successive nodes was less than four plate thicknesses. Timoshenko-beam formulas would indicate lower frequencies (and larger dampings relative to critical), but with part of the deflection resulting from shear deformation (which would not contribute to the strain at the surface of the plate).

Another criterion compares bending waves (as used in the thin-beam formulas) with shear waves (which are neglected). If the speed of a shear wave in steel were 4 km/s the plates, acting as quarter-wave resonators 254 mm long, would have a fundamental mode of shear vibration at 3937 Hz. Frequencies larger than this value obtained from thin-beam formulas are unrealistic, beginning with the fourth mode (4113 Hz) for the thicker plate and the seventh mode (5038 Hz) for the thinner plate.

It appears that special care is needed to insure that structural representations are adequate when stresses are to be an end result of calculations for structures immersed in water. Finite elements need to be small enough to delineate higher-mode vibrations or high-enough in order to include more than one mode of vibration. The effects of shear deformation and rotary inertia need to be included to represent the higher modes of thin plates properly.

Adequacy of Representation of the Fluid

The plane-wave damping used in the present calculations correctly represents the initial resistance which an acoustic fluid offers to a suddenly-started relative motion between the fluid and a structure. It persists at a particular point, however, only for the time s/c which it takes for a different pressure at a point a distance s away to be transmitted over that distance at the speed of sound c and begin to modify the plane-wave damping.

At the center of a plate 152 mm wide, for example, pressures from the sides will begin to arrive at 0.05 ms. The assumption of plane-wave radiation overestimates the damping after that time for an unbaffled plate. For frequencies up to about 5 kHz, the relatively rapid equalization of pressure on a time scale appropriate to the period of vibration allows the modes to vibrate freely as nearly-undamped systems. The plane-wave damping applies, however, to their initial response to the suddenly-applied pressure from an incident shock wave or to the abrupt inertial loading from a step acceleration of the base. Graphs displayed here illustrate responses with plane-wave damping applied for a full 1.5 ms, of which only the first 0.05 ms or so is realistic. Similar considerations apply to the presumed doubling of the incident pressure when scattering is taken as represented by simple reflection of a plane-wave.

The provision of proper representations for damping and scattering from a finite element is a difficult problem, since they depend on the shape of the element and on the influence of all the other elements in the structure. It is complicated by the fact that, as illustrated in the present simplified problem, damping regularly produces coupling among the in-vacuo modes except in special cases.

CONCLUSIONS AND RECOMMENDATIONS

The conclusions presented here are based on simplified calculations for steel plates immersed in sea water. It is believed, however, that the recommendations are applicable to fluid-structure interactions in general.

Conclusions

1. If the in-vacuo modes of vibration of a structure would be overdamped by plane-wave acoustic damping when the structure is immersed in an acoustic medium, the initial velocities and deflections of the structure in response to a shock wave in the medium or a sudden motion of the supports are controlled mainly by the damping and are less dependent on frequency or stiffness.

2. For the damping-controlled deformations, stresses and strains in the structure increase with increasing frequency or stiffness. Partial sums of strains taken for overdamped modes or strains representing overdamped deformations do not represent the true strains expected in the structure.

3. In-vacuo modes or deformations which would be lightly-damped by plane-wave acoustic damping, on the other hand, have initial deflections which are controlled mainly by frequency or stiffness. Partial sums of strains for lightly-damped modes converge rapidly to final values and strains for lightly-damped deformations are more likely to be correct estimates.

4. In the examples used here, partial sums of strains in thin plates converged to final values during the initial part of the response only if enough modes were included to bring the damping down to about 20 percent of critical for the last mode used.

5. Structural modeling to the high frequencies needed for lightly-damped modes may be difficult for steel structures in water.

Recommendations

1. If stresses or strains are important to analysis of the dynamic response of a structure immersed in an acoustic fluid, the structure must be modeled in sufficient detail to include motions which would be only lightly-damped for radiation damping.

2. Structural modeling should be appropriate to the frequency range needed to reach the lightly-damped regime.

3. For example, in the case of thin steel plates struck by a plane shock wave in sea water, from 8 to 20 in-vacuo modes were needed to obtain convergent values for initial bending strain. Modes having plane-wave damping down to about 20 percent of critical were included. The thin-beam formulas which were used to calculate the modes of the plates were not adequate for the range of modes which had to be included.

REFERENCES

1. R. W. Hamming, "Numerical Methods for Scientists and Engineers," New York, New York. McGraw-Hill Book Company (1962).

2. G. J. O'Hara, "Shock Spectra and Design Shock Spectra," Washington, DC. Naval Research Laboratory NRL Report 5386 (November 12, 1959).

3. L. P. Petak and R. E. Kaplan, "Resonance Testing in the Determination of Fixed Base Natural Frequencies of Shipboard Equipment," Washington, DC. Naval Research Laboratory NRL Report 6176 (December 15, 1964).

4. G. J. O'Hara and L. P. Petak, "The Effect of a Second Mode and Nearby Structures on Shock Design Values," Washington, DC. Naval Research Laboratory NRL Report 6676 (April 5, 1968).

5. R. S. Schechter and R. L. Bort, "The Response of Two Fluid-Coupled Plates to an Incident Pressure Pulse," Washington, DC. Naval Research Laboratory NRL Memorandum Report 4647 (October 12, 1981).

6. G. J. O'Hara and H. Huang, "Yielding Effects on Design Shock Spectra," Washington, DC. Naval Research Laboratory NRL Memorandum Report 3862 (September 1978).

7. L. W. Fagel, "Acceleration Response of a Blast-Loaded Plate," The Shock and Vibration Bulletin, Bulletin 42 Part 2 pages 221 to 233 (January 1972).

8. W. F. Hartman, "Acceleration Response of a Blast-Loaded Plate," The Shock and Vibration Digest Volume 5 Number 2 page 63 (February 1973).

9. R. L. Bort, S. M. Halperson, and A. V. Clark, "Underwater-Explosion Tests of Simple Structures with Appendages Attached," Washington, DC. Naval Research Laboratory NRL Report 7796 (October 25, 1974).

10. Mario Paz, "Structural Dynamics Theory and Computation," New York, New York. Van Nostrand Reinhold Company (1980).

END

FILMED

9-83

DTIC